Hindawi
Advances in Civil Engineering
Volume 2022, Article ID 3178269, 14 pages
https://doi.org/10.1155/2022/3178269

Research Article

Optimization and Prediction of Energy Consumption, Daylighting, and Thermal Comfort of Buildings in Tropical Areas

Jianjian Zhang[1] **and Lin Ji**[2]

[1]*Macau Institute of Systems Engineering, Macau University of Science and Technology, Macau 999078, China*
[2]*School of Business, SEGi University, Kuala Lumpur 47810, Malaysia*

Correspondence should be addressed to Jianjian Zhang; 771022886@qq.com

Received 27 October 2021; Revised 20 January 2022; Accepted 17 February 2022; Published 27 March 2022

Academic Editor: Sandra Cunha

Copyright © 2022 Jianjian Zhang and Lin Ji. This is an open access article distributed under the Creative Commons Attribution License, which permits unrestricted use, distribution, and reproduction in any medium, provided the original work is properly cited.

As awareness of the ecological environment and sustainable development has increased, green buildings have received significant attention in the design stage. For the initial design stage of buildings in the tropics, cooling energy consumption, daylighting, and thermal comfort are necessary steps for green and energy-saving design. Therefore, this study focuses on three objectives: (1) cooling load, (2) useful daylight illuminance (UDI), and (3) the predicted mean vote (PMV). First, this research uses Rhino3D and the Grasshopper plug-in to build an architectural model and uses the Octopus plug-in in Grasshopper to iteratively calculate the target value to solve the multiobjective balance problem and find the relative optimal value. Next, the optimized design value is compared with the initial solution, and the cooling energy consumption is reduced by 7.48%–7.76%, the UDI increases by 0.44%–2.07%, and the PMV is reduced by 25.67%–27.43%. It is shown that the optimized layout of the office achieves energy-saving optimization in energy consumption, daylighting, and thermal comfort. Finally, the backpropagation (BP) neural network established in this research is shown to achieve good prediction of the target value and achieves the goal of green energy-saving.

1. Introduction

The world is currently in a stage of rapid industrialization and urbanization, and building energy consumption has increased significantly year by year. In 2018, the final energy used by the global construction industry for buildings and operations accounted for 36% of final energy use [1]. In the same year, China's total construction area reached approximately 60.1 billion square meters, of which the urban residential construction area was 24.4 billion square meters [2], and China's building and operating energy consumption accounted for 37% of the total energy consumption of the whole society. Therefore, optimizing building energy-saving design and reducing building energy consumption have become measures for China to cope with the increase in total energy consumption. The world is working together to create a healthy and environmentally friendly living environment on the premise of reducing resource consumption and improving resource utilization efficiency. Reducing the threats of environmental pollution and ecological destruction and realizing the sustainable use of resources have become urgent problems to be solved.

In recent years, there have been numerous studies and applications in the construction industry to develop green buildings with low energy consumption as the core [3, 4]. Because it is difficult for design researchers to have extra time to study complex simulation software to explore the best solutions for energy consumption and daylighting, researchers have introduced multiobjective optimization methods to improve multiple performance goals of buildings [5]. They use multiobjective evolutionary algorithms to observe the impact of changes in independent variables on multiple performance goals and select the best independent variables to determine the optimal solution [6]. In the selection of an evolutionary algorithm, owing to the good global search ability of genetic algorithms [7], many scholars use them as a tool for energy-saving optimization of green buildings [8]. In the selection of research goals, scholars

mostly conduct research on the sustainable development of energy consumption and daylighting performance.

Toutou et al. [9] used the Grasshopper plug-in in Rhino3D to simulate the daylighting and energy consumption of the building model and used a genetic algorithm executed by the Octopus plug-in to optimize the building parameters, such as window-to-wall ratio (WWR), building materials, glass materials, and shading devices, so as to achieve the best performance of the building in terms of daylighting and energy performance. Fang and Cho [10] used parametric design to construct simulation models and used genetic algorithms to optimize building performance, which can help designers evaluate daylighting and energy consumption at the same time and generate optimized design effects. The parameters evaluated include the geometry of the building, the width and length of skylights, the length of shutters, and climatic conditions. In 2013, Lartigue et al. [11] used the WWR and the window type as decision variables to optimize the heating load, cooling load, and daylighting performance of the room. Zhang et al. [12] optimized the orientation, room depth and corridor depth, WWR of different interfaces, glazing materials, and shading types to achieve the minimum heating and lighting energy consumption, minimum summer discomfort time, and maximum useful daylight illuminance (UDI) of typical classrooms in cold regions of China.

On the basis of the above mentioned research, some scholars consider the cost factors in the objectives. Han et al. [13] established a simulation-based multiobjective optimization model by optimizing building width, roof height, WWR, window height, and orientation. They aimed to improve the daylighting, energy efficiency, and economic performance of wooden and glass buildings in severe cold areas. Some scholars added indoor thermal comfort to the objectives. Lakhdari et al. [14] used a genetic algorithm in the Grasshopper parametric modeling tool to automatically modify the parameters of the enclosure structure, such as WWR, wall materials, glass types, and shading devices, which improves UDI, adaptive thermal comfort, and energy efficiency. Zhu et al. [15] used Grasshopper to establish three benchmark models of rural tourism buildings (RTB). A multiobjective optimization tool was used to select RTB shape and WWR as variables to achieve the best performance in energy consumption, indoor daylight, and thermal comfort. Zhai et al. [16] proposed a multiobjective optimization method to optimize energy consumption, daylighting, and thermal performance through various window parameters.

The above description demonstrates that the research target usually selects the energy consumption, daylighting, cost, and other related properties of the building, while the independent variables are usually WWR, building materials, shading devices, and sizes. This passive building energy-saving design method has changed the design process of researchers and architects relying on design experience. It provides a scientific basis for designers to obtain more reasonable and energy-saving residential building design schemes. Based on previous studies [13–17], cooling load, UDI, and predicted mean vote (PMV) are utilized in this study as objectives in tropical regions of China. Compared with residential buildings, office buildings have higher daylighting requirements and a large proportion of open windows, which results in a greater reduction of energy consumption and comfort [18]. Therefore, office buildings are considered as the research object in this study. At the same time, this study achieves the following innovations:

(1) This study considers the number of horizontal panels, depth, and angle [19] of the building shading device louver together with the traditional WWR and window height for independent variable optimization analysis [9]. The rationality of the design of the tropical area's louver leaves has a great influence on the indoor energy consumption, daylighting, and thermal comfort index PMV [20].

(2) This study proposes a multiobjective optimization design method based on backpropagation (BP) neural networks [21] to quickly and accurately predict the energy consumption, daylighting, and thermal comfort of residential buildings.

(3) Because there are few studies on multiobjective optimization of energy-saving in buildings in this region at this stage, and office buildings require high daylighting and large WWR, thus, this study takes the energy consumption, daylighting, and thermal comfort of office buildings as the target, which has innovative technical research and guiding significance for reducing high energy consumption and improving effective daylighting in this area [18].

The remainder of this paper is organized as follows. Section 2 introduces the mathematical model of multiple objective functions. Section 3 introduces the experimental setup and optimization process. Section 4 presents the optimization results and discussion. Finally, Section 5 summarizes the study.

2. Materials and Methods

2.1. Objective Functions

2.1.1. Useful Daylight Illuminance. UDI is a dynamic natural lighting evaluation index proposed by Nabil and Mardaljevic based on the illuminance value of the working plane [22]. It refers to the proportion of the time of natural light in the effective illuminance range on the working plane in the whole year. UDI can be divided into three ranges: the value between 100 and 2000 lx indicates that the natural light of the location is effective; the value less than 100 lx indicates that the natural lighting level is insufficient; and the value greater than 2000 lx causes visual discomfort and glare. Therefore, this study chooses 100–2000 lx as the satisfactory range of solar calculation of UDI and maximizes UDI [23].

2.1.2. Thermal Comfort. This refers to the comfort of the human body to the surrounding thermal environment.

Specifically, it means that there is heat transfer and flow between the human body and the surrounding environment and a dynamic balance is achieved in this process. In the objective environment, variables such as dry bulb temperature, wind speed, and humidity have an impact on human thermal comfort. The comfort degree of the indoor thermal environment is one of the main factors affecting people's health, as well as work and learning efficiency [24]. In order to obtain a more comfortable thermal environment, this paper selects the most widely used thermal comfort evaluation index PMV to measure the indoor thermal comfort of buildings, which as displayed in Table 1. Because the region is tropical and the PMV is greater than 0 all year round, one of the objectives of this paper is to minimize PMV.

Because the research object is the tropics, the energy consumption of buildings in this area is mainly the energy consumption of air conditioners. While the heating load is essentially zero, and the energy consumption of electrical equipment and lighting changes little, this paper only considers cooling load as the energy target [25]. Therefore, the optimization goal of this paper is to minimize the cooling load, PMV, and to maximize UDI. Since the Octopus plug-in can only perform the minimization operation, it is sufficient to add a minus sign in front of equations, as shown in

$$\min \begin{cases} -f_{\mathrm{UDI}}(x), \\ f_{\mathrm{PMV}}(x), \\ f_{\mathrm{cooling\,load}}(x). \end{cases} \tag{1}$$

2.2. Constraint Functions and Variables.

$$\begin{cases} \mathrm{WWR} \le 0.4 & (a), \\ 2\,\mathrm{m} \le \mathrm{Window\ height} \le 4.5\,\mathrm{m} & (b). \end{cases} \tag{2}$$

This paper aims to obtain a more comprehensive analysis of the target value, but the building is located in the tropics, so that it is hot all year round. When the proportion of WWR is too large, the energy consumption of indoor air-conditioning will greatly increase. Therefore, in this paper, it is necessary to consider the scope of WWR. On the basis of meeting the requirements of public building codes [26], this research makes WWR not more than 0.4. For the constraint setting of window height, because the height of this floor is 4.5 m, the upper limit of the window height is set to 4.5 m. When designing the minimum value of window height, the overlap between windows caused by the maximum WWR should be considered. When the maximum WWR is 0.4 and the window height is only 2 m, the windows just overlap each other, so that the lower limit of window height is set to 2 m. The constraint function derived from the above code is expressed by (2).

The specific WWR range is set according to the actual situation and constraints of building windows; thus, the WWR is set in four directions from 0.1 to 0.4, as shown in Table 2. In addition, the building shading device louver [27] is shown in Figure 1. It is determined by three independent variables: the number of horizontal panels of the louver, the louver depth, and the louver angle. The specific variation range of louvers is shown in Table 2.

3. Case Study

3.1. Location and Climate. The location of the research object is Sanya, China, which belongs to the tropical region and the ocean monsoon climate zone. In terms of temperature, the annual average temperature is 25.4°C, the average temperature of the coldest month is 23°C, the average temperature of the hottest month is 29.7°C, and the annual sunshine hours are up to 1950–2950 h. The area faces frequent typhoons and alternating wet and dry conditions. The annual average rainfall is 1190 mm, and rainfall is concentrated from May to October, accounting for 75% to 90% of the annual rainfall. The detailed climate information of Sanya should be based on the US Department of Energy's weather data; however, there is no relevant information in the database. Therefore, the climate information is based on that of Dongfang, which is 168 km away from Sanya, as shown in Figure 2, and the climate information is listed in Table 3.

3.2. Equipment and Measurements. In order to verify the authenticity and effectiveness of the climate simulation, the outside temperature and humidity of Sanya were measured using a JT2020 Multifunction Tester, which is shown in Figure 3(a). The temperature measurement range is −20°C to 120°C with an accuracy of ±0.5°C. The humidity measurement range is 10% to 95%, and the accuracy is ±3%.

The specific test time of this study is January 7th and 9th, 2022, and the simulation and test of temperature and humidity take the average of these two days. The temperature test results and simulation results are shown in Figure 3(c). The average difference between the two is 2.46, the standard deviation is 0.64, and the variance is 0.41. The test and simulation results of humidity are shown in Figure 3(d). The average difference between the two is 2.21, the standard deviation is 2.20, and the variance is 4.83. Since the Dongfang and Sanya are not in the same place, there is a certain error in the results, but the climates of the two places are still very close. Therefore, the climate simulation of the Dongfang used in this study is real and valid.

In Figure 3(b), a DT-1332A Digital Illuminance Meter is used for illuminance measurement. The measuring range of the equipment is 0.1–200000 lx, and the accuracy is ±3% rdg. ± 0.5% f.s. In this study, a local office was selected for reflectance measurement. The decoration of the office is close to the white emulsion varnish wall and floor tiles selected for the project. Finally, the average reflectance of white emulsion varnish on four sides of the office was measured to be 0.83, and the standard deviation was 0.05, which was close to the parameter of 0.84 selected in this study [28], so the parameter is reliable. In this study, the average reflectivity of the floor tiles at 6 uniformly dispersed points in the office is 0.51, and the standard deviation is 0.02, which is close to the simulation parameter 0.53 selected in this study [28]. The above measured values verified the accuracy of the parameters selected for the daylighting simulation.

Table 1: Level 7 indicators of PMV.

PMV value	+3	+2	+1	0	−1	−2	−3
Thermal comfort	Heat	Warm	Slightly warm	Moderate	Slightly cool	Cool	Cold

Table 2: Design variables and ranges of values.

Type	Material	Parameter	Range
Window	6C_12A_6C glass	WWR of north	$0.10 \le \text{WWR} \le 0.4$
		WWR of west	$0.10 \le \text{WWR} \le 0.4$
		WWR of south	$0.10 \le \text{WWR} \le 0.4$
		WWR of east	$0.10 \le \text{WWR} \le 0.4$
		Window height	From 2.0 to 3.5 m with 0.1 m increment
Shading material	Aluminum	Number of horizontal panels of louver	From 5 to 20 with 1 increment
		Depth of louver	From 0.03 to 0.10 m with 0.01 increment
		Angle of louver	From −60° to 60° with 10° increment

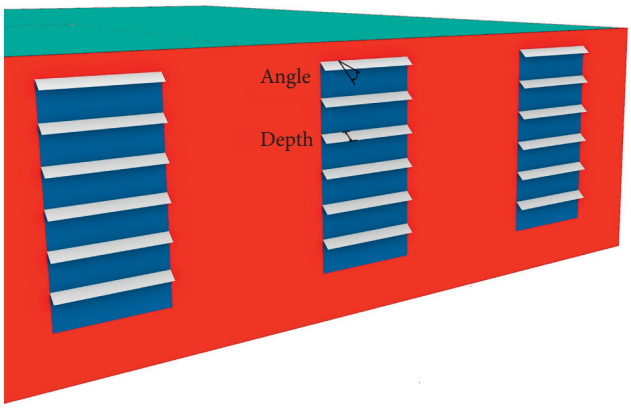

Figure 1: Layout of louver depth and angle.

Figure 2: Location of Sanya, Dongfang, and Beijing on a map of China.

3.3. Geometry. There are three buildings in the project, and the research building is the south breeding science and technology service center in the north, which can be seen in Figure 4(a). The building structure is a reinforced concrete frame structure with a building height of 50.7 m, which is divided into 1 floor underground and 11 floors above ground; the total construction area is 20909 m^2, and its specific size is $107.05 \times 24.5 \times 50.7$ m^3.

Considering the efficiency and time of computer operation optimization, this paper selects one of the layers for analysis. In addition, since the building from the 1st floor to the 2nd floor is a nonstandard floor, the 3rd floor to the 11th floor is a standard floor, and the 7th floor belongs to the middle floor of the standard floor of the building, so that the 7th floor is selected as a representative for analysis, and the optimized results can provide better reference data for the upper and lower floors. The boundary conditions of the 7th floor analyzed in this study are the elevation of 28.2 m and the floor height of 4.5 m. There are three equipment rooms and eight offices, of which there is a multifunctional office at the east and west ends. A 16.8 m long outdoor corridor, a mid-air atrium, and a rest platform are set on the west side of the east elevator. The detailed layout information is shown in Figure 4(b). The atrium is set to be hollow, and the external corridor and rest platform are composed of enclosures with lower elevations. The stairwell is merged into a closed room.

3.4. Tools and Optimization Method

3.4.1. Modeling Settings. Firstly, this paper use Rhino3D to build the office model, embeds the model into the module (Honeybee_Mass2Zones), and then introduces it into the module (Honeybee_Glazing, based on ratio). In the initial settings, this case is based on design experience and sets the WWR on the north, west, and east sides as 0.2, the WWR on the south side as 0.3, the window height as 3 m, and the number of horizontal panels of the louver as 10, and the louver depth and angle are 0.07 m and 0°, respectively.

3.4.2. Materials Setting. Since this paper does not consider material variables, it is assumed that the real material and the assumed material have the same total thermal resistance and the R-value is shown in Table 4. The window selected is (6clear_12air_6clear) glass [29] as the window material, and the EP parameters are listed in Table 4. Table 5 displays the radiation properties of the indoor white emulsion varnish,

Table 3: Climate information of Dongfang.

Parameter	Avg. dry bulb temp (°C)	Max temp (°C)	Min. temp (°C)	The percent of temperature over 26°C (%)	Avg. relative humidity (%)	Avg. wind direction (°)	Avg. wind speed (m/s)
Value	25.23	33.8	12.5	49.06	78.19	130.03	4.26

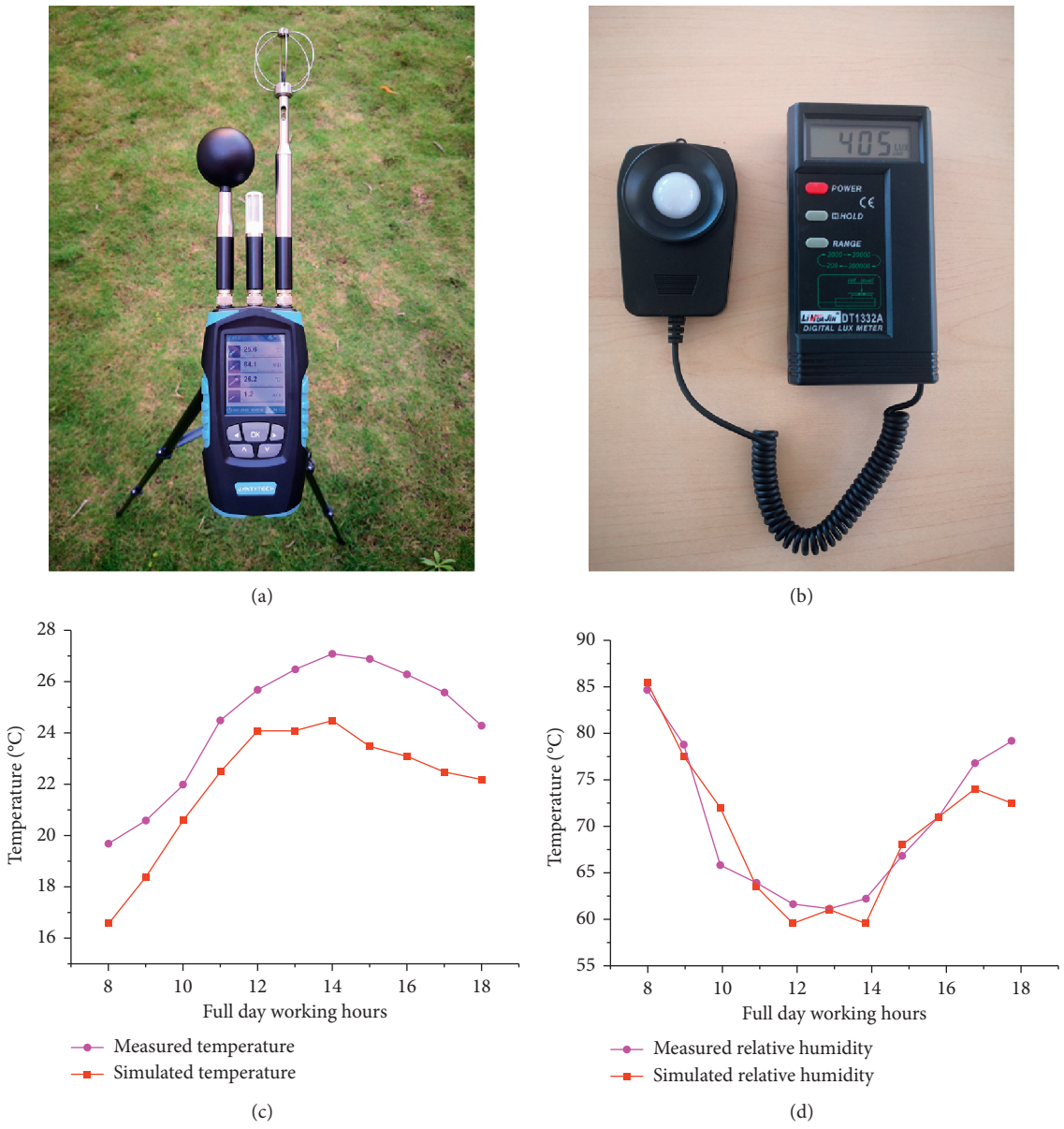

Figure 3: Actual measured and simulated temperature, humidity, and measured illumination. (a) Temperature and humidity tester is JT2020 Multifunction Tester; (b) tester is DT-1332A Digital Illuminance Meter. (c) and (d) Comparison between real temperature and humidity and simulated temperature and humidity on January 7 and 9, 2022.

floor tile, and glass, which can accurately reflect the indoor illumination environment [28]. Aluminum has the advantages of energy-saving and environmental protection; thus, aluminum is selected as the shading devices, and the parameters are listed in Table 6 [28, 30].

3.4.3. Energy Parameter Settings. In the zone of energy parameter thresholds of Sanya, it is necessary to consider the cooling demand. The cooling temperature is set to 26°C; equipment load is set to 15 W/m^2; lighting density is set to 10 W/m^2; and number of people per area is set to 0.1, as displayed in Table 7.

In this study, OpenStudio is selected for energy consumption simulation, and Ideal Air Loads is selected for cooling in the HVAC system. A schedule is introduced to divide weekly work and rest periods by taking into account

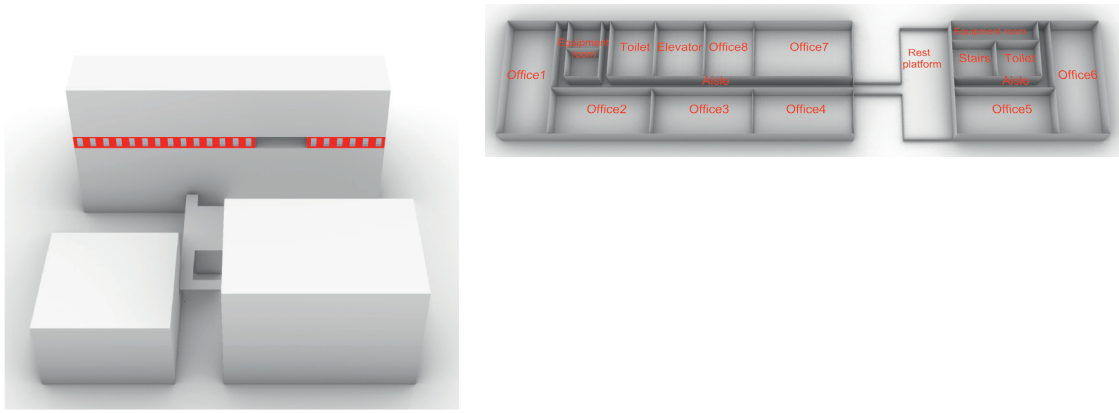

(a) (b)

Figure 4: Location map of Southern Breeding Technology Service Center. (a) Overall location map of the project and (b) functional layout of the 7th floor of the project.

Table 4: Material information of EP construction from wall and glass.

Parameter	EP transparent material	
	Exterior wall	6clear _12air_6clear
R-value (m^2·K)/W	1.3	
U-value W/(m^2·K)		2.59
Thermal solar heat gain coefficient (SHGC)		0.75
Visible transmittance (VT)		0.81

Table 5: Material information of radiation from opaque radiation material and glass.

Parameter	Opaque radiation material		Transparent radiation material	
	White emulsion varnish (wall)	White emulsion varnish (ceiling)	Floor tile	6clear _12air_6clear
Reflectance (RGB)	0.84	0.84	0.53	
Transmittance (RGB)				0.81
Refractive index				1.52
Roughness	0.15	0.15	0.05	
Specularity	0.03	0.03	0	

Table 6: Material information of louvers.

Parameter	Aluminum
Reflectance (RGB)	0.88
Roughness	0.02
Specularity	0.5

Table 7: Zone energy parameters.

Member	Parameter	Value
EP zone loads	Equipment load	15 W/m^2
	Light density	10 W/m^2
	Number of people	0.1 ppl/m^2
EP zone thresholds	Cooling set point	26°C
HVAC system	Ideal air loads	-

employees' normal work and rest periods. In Figure 5, red means work, blue means rest, and yellow means that both are possible [31]. Specifically, the working hours of Sanya are five days per week, and the daily working hours are 8 am to noon and 3 pm to 6 pm. There are also two major festivals with public rest for seven days: the Spring Festival in January or February and the National Day on October 1, as well as some public rest days, such as New Year's Day and Labor Day on May 1.

3.5. Integration Process. Rhinoceros (Rhino3D, Robert McNeel & Assoc., USA) is 3D modeling software that can use geometric modeling platforms to build complex building shapes and space. Grasshopper is a plug-in for Rhino3D that runs under the Rhino3D environment, which includes Ladybug and Honeybee, Octopus, Butterfly, and Human extended platforms. The Ladybug and Honeybee plug-ins are important computing platforms [32, 33], which can call the required device and material data before the building energy simulation. They can also call the device and material information before the daylight is simulated. Radiance, EnergyPlus, OpenStudio, and other external software can be used to simulate natural daylight, thermal engineering, and other parameters.

In this study, we use Grasshopper software to build a 3D model of the project and then use Ladybug and Honeybee plug-ins to simulate the energy consumption, daylighting, and PMV performance. The genetic

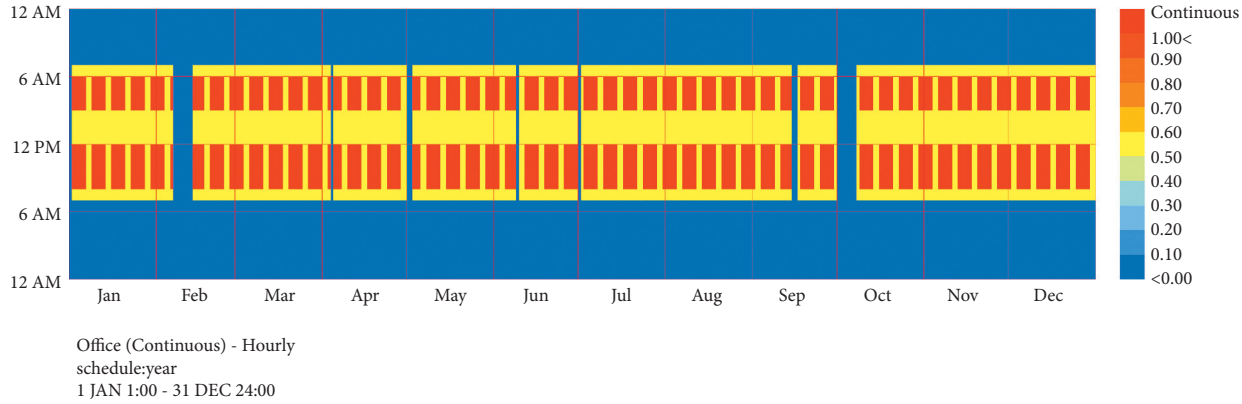

Figure 5: Sanya's annual work and rest schedule.

algorithm encapsulated by the Octopus plug-in is then used to optimize the design parameters to achieve the goal of multiobjective optimization [32]. Finally, the multiobjective prediction of the cooling load, UDI, and PMV is carried out through the alternative model formed by the BP neural network, which enables architects to evaluate and predict the target value more quickly. The whole process is shown in Figure 6.

4. Results and Discussion

4.1. Single Variable Analysis. Before multiobjective optimization, a single variable is first compared and analyzed. In all the initial settings, the WWR on the north, west, and east sides are set to 0.2, the WWR on the south side is set to 0.3, the window height is set to 3.0 m, and the number of horizontal panels, depth, and angle of a louver are set to 10, 0.07 m, and 0°. In Figure 7(a), the representative south WWR is selected as the variable, which increases from 0.1 to 0.4 (increment of 0.05), and the other independent variables remain unchanged. It can be seen from the results that UDI increases from 72.31% in the initial stage to 74.54% and then decreases to 69.48% in the later stage. The increase in UDI is due to the increase in WWR; the original illuminance value was lower than 100 lx and reached the range of 100 to 2000 lx, which leads to an increase in UDI. In the later period, part of the illuminance value exceeds 2000 lx, which leads to a decline in UDI. For the cooling load, due to the increase of WWR, the indoor solar heat gain increases [34], and the corresponding window thermal resistance R is smaller than the wall, which results in an increase of the cooling load from 167.71 kwh/m^2 to 181.15 kwh/m^2. This result is similar to the study by Xue et al. [35] that the energy consumption increases with the increase of WWR and the change trend increases linearly. In the same way, PMV increases from 0.92 to 1.23 and then stabilizes. It can be seen from Figure 7(a) that the increase of WWR on the south side leads to an increase of energy consumption and PMV value, which is not conducive to reducing energy consumption and indoor comfort. Therefore, the WWR on this side should be reduced in the design.

In Figure 7(b), when the other variables are at the initial settings and the window height is from 2.0 m to 3.5 m (increment of 0.2 m), it has little effect on UDI, but it causes the cooling load to increase from 173.49 kwh/m^2 to 177.63 kwh/m^2. At the same time, the PMV value increases from 1.18 to 1.21 and then decreases to 1.10. The PMV tends to be beneficial as the window height increases; thus, the design of the window height should consider the cooling load and PMV value comprehensively.

In Figure 7(c), when the other variables are at the initial setting values and the number of horizontal panels of the louver is increased from 5 to 20 (increment of 3), the illuminance value increases slightly in the range of 100–2000 lx, which increases UDI from 72.09% to 72.35%. When the building is being cooled, as the number of horizontal panels increases, it blocks solar radiation directly into the building, which in turn reduces indoor solar heat gain [36]. Therefore, it reduces the cooling load from 180.05 kwh/m^2 to 169.05 kwh/m^2 and the PMV from 1.15 to 1.08. Overall, this variable favors three goals. It can also be seen from Figures 7(d) and 7(e) that the influence of the depth and angle of the louver on the target is similar to that of Figure 7(c).

It can be seen from the above analysis that a smaller WWR is beneficial to UDI, while the other four independent variables make UDI change steadily within a certain range. The cooling load and PMV value increase significantly with the increase of WWR; however, the two objects decrease with an increase of the horizontal panels, length, and angle of the louvers. At the same time, an increase in the height of the window is only beneficial to the PMV. Therefore, the comprehensive analysis of the single-target results in this paper shows that reducing WWR, increasing the louver's horizontal panel number, depth, angle, and appropriate window height are conducive to the three research goals for achieving good results.

4.2. Multiobjective Optimization Results and Analysis. Through comprehensive consideration, this paper sets the objectives as cooling loads, UDI, and PMV. The Octopus plug-in was used to call the intelligent optimization algorithm; the WWR, window height, and louvers were selected as independent variables. According to the complexity of this study, population size is set to 20 and other settings are

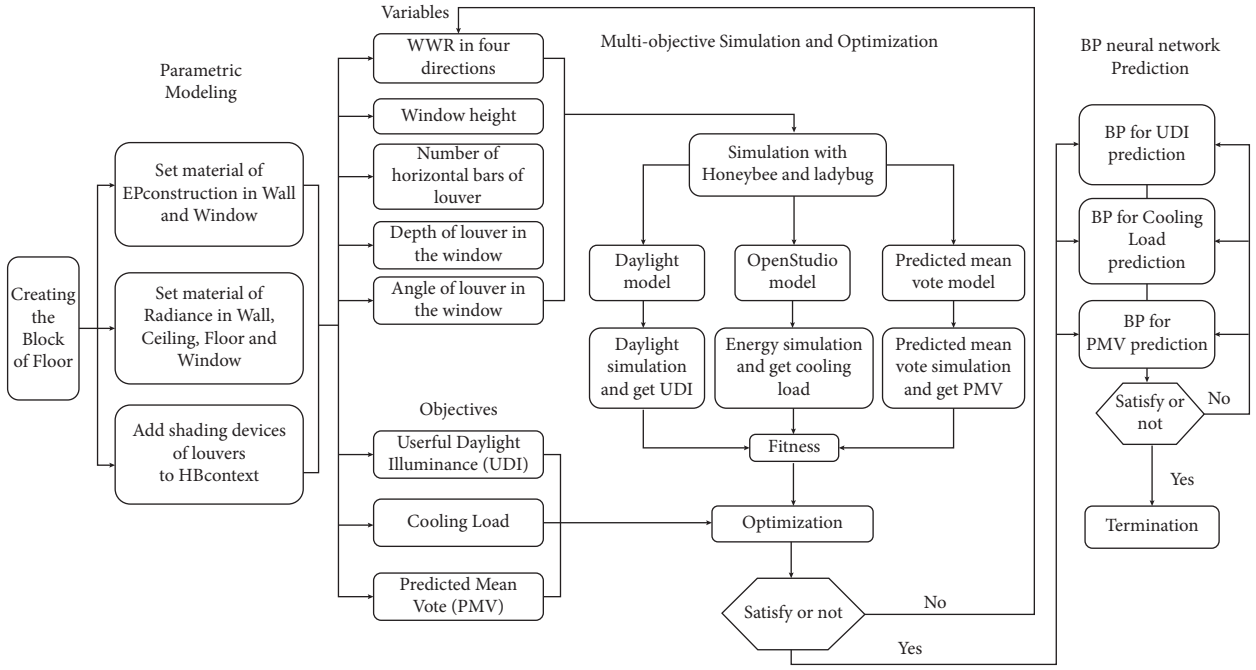

Figure 6: Optimization process of the simulation.

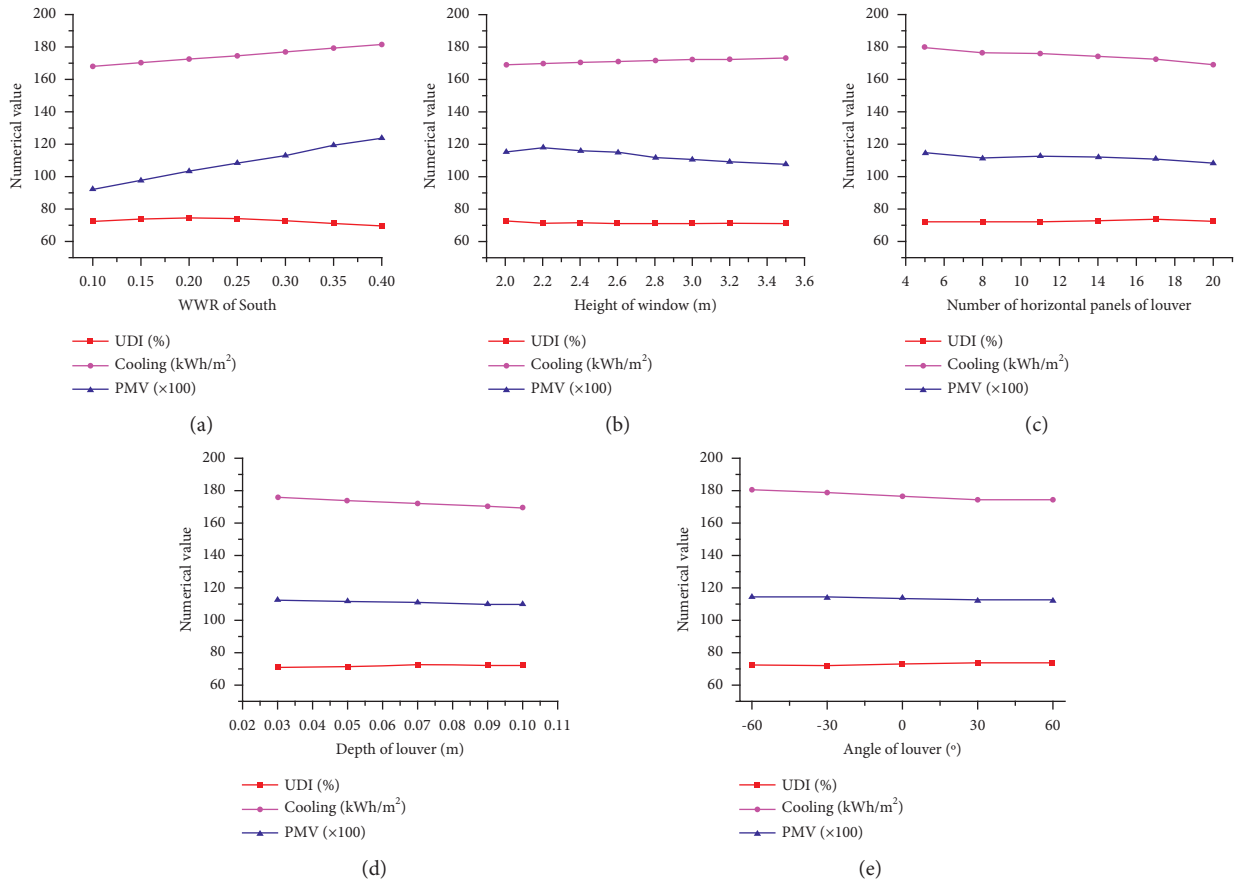

Figure 7: Influence of independent variable on three target values. (a) Target value change is caused by the WWR variable on the south side; (b) window height variable causes the target value to change; (c, d, e) number of horizontal panels, depth, and angle of louvers cause the target value to change.

set to default values. The three goals are unable to achieve the best value at the same time; therefore, a balance among the goals needs to be found.

After 51 generations of iterative calculations, the entire optimization process is essentially in a stable state; thus, the optimization data of the previous 51 generations are selected for analysis. The 51st generation Pareto frontier is shown in Figure 8.

In the 51st iteration of this building, the nondominant solution set corresponding to UDI and cooling load is nonlinear and is negatively correlated, as shown in Figure 9. When UDI increases from 63.43% to 77.57%, the cooling load shows an increasing trend, increasing from 161.30 kwh/m^2 to 168.47 kwh/m^2. This is due to the increase of WWR in the north-south direction, which increases the solar heat gain. In addition, the indoor thermal resistance R of the corresponding position decreases, which leads to a continuous increase of the cooling load and UDI. At this time, the variables of the louvers and the height of the windows all change in a certain range, so that the mutual factors should be considered when optimizing the variables.

The relationship between UDI and PMV is shown in Figure 10. When UDI increases from 63.43% to 77.57%, PMV also shows an increasing trend, and the PMV stabilizes at approximately 1.05 in the later period. This is mainly due to the increase of the WWR of the north-south windows, which promotes the increase of indoor solar heat gain, thereby increasing the indoor illuminance and the indoor uncomfortable area, which in turn leads to an increase in the PMV value and UDI. UDI is increased to 77%, due to WWR on the north side increasing to a very large ratio of 0.37 to 0.4, resulting in a PMV value of approximately 1.05, which in turn causes the PMV value to present an interval change in the leftmost area. The two are negatively correlated as a whole; thus, the factors restricting each other when optimizing should be considered.

The relationship between cooling energy consumption and PMV is shown in Figure 11. When the cooling load value increases from 161.30 kwh/m^2 to 168.47 kwh/m^2, the PMV increases from 0.74 to 1.07. These two goals are mainly due to the increase of indoor solar heat gain with the increase of WWR on the north and south sides, resulting in an increase in indoor uncomfortable areas and cooling energy consumption. Therefore, cooling energy consumption is positively correlated with PMV. Therefore, from the comparative analysis of the above three goals, UDI and cooling load are negatively correlated, UDI and PMV are also negatively correlated as a whole, and cooling load and PMV are positively correlated as a whole. Therefore, the influence of all objective functions in the design process should be considered.

Through the comparison and analysis of the various goals of the 51st generation, three relatively optimal nondominant solutions are selected, which causes the office area of the floor to have better energy-saving performance [17]. Table 8 lists the target values and corresponding independent variables of the three solutions. Compared with the initial solution, the UDI values of the optimal solutions increase slightly, from 72.59% to 72.91%–74.09%, with an

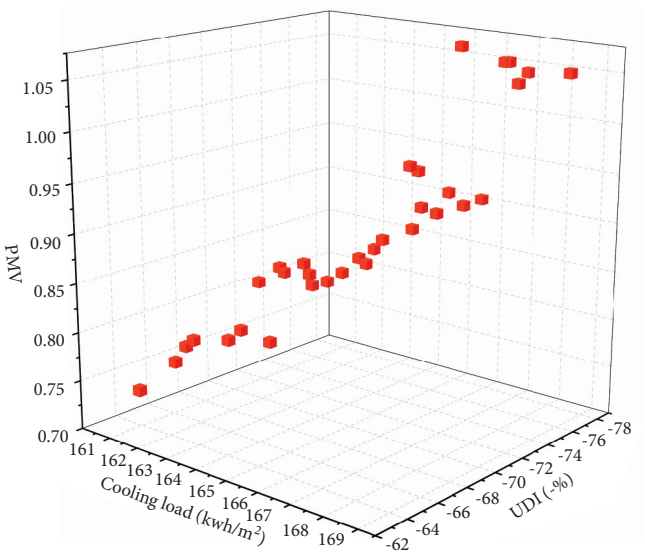

Figure 8: Nondominated solutions of the three objectives in the 51st iteration.

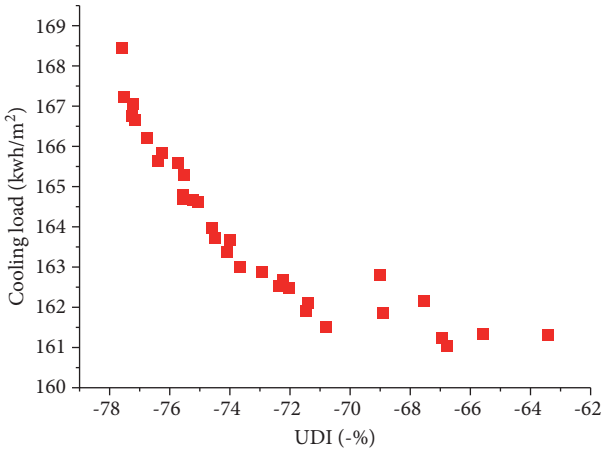

Figure 9: UDI and cooling load performance of nondominated solutions in the 51st iteration.

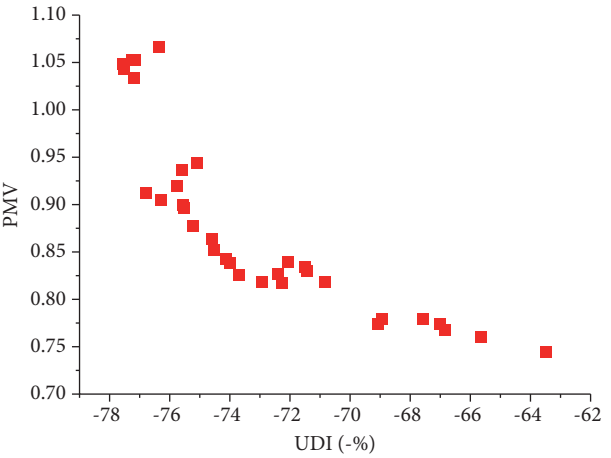

Figure 10: UDI and PMV performance of nondominated solutions in the 51st iteration.

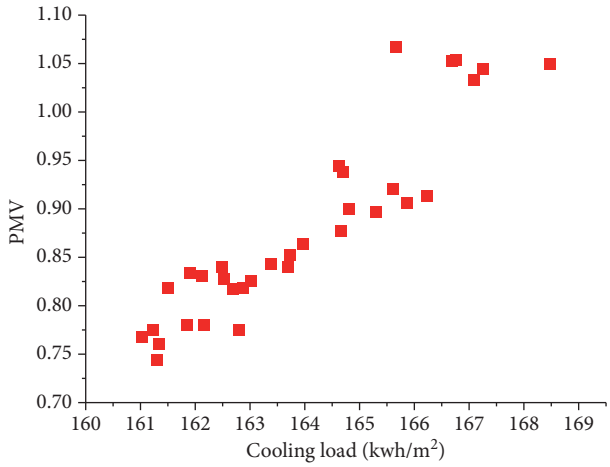

Figure 11: Cooling load and PMV performance of nondominated solutions in the 51st iteration.

increase of 0.44%–2.07%; the reductions in energy consumption are obvious, which are reduced from 176.58 kwh/m^2 to 162.87–163.38 kwh/m^2, and from October of that year to March of the following year the average monthly decrease reaches approximately 20%. The PMV values are reduced from the initial value of 1.13 to the range of 0.82–0.84, that is, a decrease of 25.66%–27.43%. Rana et al. achieved energy savings of 9.40% in the existing office building by adopting the optimal proportion of WWR; the cooling energy consumption in this study was ultimately reduced by 7.48%–7.76%, which is similar, and the daylighting and thermal comfort of this study have been improved too [34]. Compared with the study by Nasrollahzadeh, its energy consumption and daylighting have been greatly improved, and the discomfort percentage PPD has been reduced by only 14%, while the PMV in this study has been reduced by 25.67%–27.43%, which makes the office staff have a more comfortable office environment [37]. Therefore, it can be seen from the above analysis that the optimized layout of the building has achieved very good improvements in energy consumption, daylighting, and thermal comfort and can effectively achieve the energy-saving optimization of the building.

In this study, daylight simulation is used to calculate UDI of the initial solution and options; from the three Pareto fronts listed in Table 8, it can be seen that the target values of Options 1, 2, and 3 are optimized compared with the initial solution. However, the UDI improvement of Option 2 is relatively small, so that Options 1 and 3 are compared again. Although the improvement of the target value of UDI of Option 1 is not as good as that of Option 3, the two other target values have been optimized more than Option 3; thus, the initial solution and Option 1 are selected for comparative analysis, and daylight simulation is used to calculate the initial solution and the UDI of Option 1. The visualization results are shown in Figure 12.

The average UDI of the initial solution in Figure 12(a) is 72.59%, and the average UDI of Option 1 in Figure 12(b) is 73.67%, which increases by 1.49% after optimization. It can be seen that the effective illuminance value of the north side of Option 1 is essentially unchanged after optimization. However, with the decrease of WWR on the west, south, and east of the side and the increase of horizontal panels and length of the louvers, the illuminance values of more than 2000 lx near the window and some middle areas in these three directions are reduced to the effective range of 100–2000 lx, so that the effective illuminance value is distributed from the inner side to the middle and the position near the window. The optimization makes the UDI distribution in these three directions more uniform and reasonable and overall has a certain improvement compared with the previous one.

In this paper, the PMV analysis and calculation are carried out for the initial solution and Option 1, respectively [33]; the visualization results are shown in Figure 13. The PMV value of the initial solution in Figure 13(a) is 1.13, and the PMV value in Figure 13(b) is 0.83, which is reduced by 26.55% compared with the initial value. The optimized value significantly improves the indoor comfort. Specifically, the PMV value on the north side of Option 1 is basically unchanged, but, in other directions, with the decrease of WWR and the increase of horizontal panels and depth of louvers, the illuminance values near windows and middle areas on the west, south, and east sides are reduced, leading to a decrease in indoor solar heat gain, which improves the indoor thermal comfort, so as to make the PMV in these three directions reach a more ideal state.

4.3. Regression Analysis. In order to solve the time-consuming problem of optimization of the three target values, this study uses MATLAB (MathWorks, USA) for analysis and utilizes a BP neural network to predict the target value. Firstly, the building parametric modeling platform is constructed based on Rhino3D and Grasshopper, and then the platform is used for target simulation and optimization. It then extracts the independent variables and target data in the optimization process and constructs the BP neural network multiobjective optimization model through MATLAB. Finally, the trained neural network model is predicted.

In this paper, 1157 independent variables and corresponding objective function values obtained from 51 generations of operation are imported into MATLAB to test the prediction accuracy of the alternative model. The neural network adopts a three-layer model, the number of design parameter variables is 8, the number of target samples is 3, and the number of hidden layer nodes is 12. Therefore, the best network topology of the alternative model is $8 \times 12 \times 3$. In addition, 1157 groups of data are randomly assigned, and the sample is divided into two parts: 90% for training and 10% for testing. In addition, the sample training data are normalized. The linear correlation coefficients of training samples, verification samples, test samples, and all samples are close to unity, which shows that the BP neural network established in this study can achieve good prediction after training.

Table 8: Comparative analysis of Pareto optimal solutions and initial solution.

Office room style	Initial solution	Option 1	Option 2	Option 3
WWR of north	0.2	0.2	0.19	0.22
WWR of west	0.2	0.11	0.11	0.11
WWR of south	0.3	0.1	0.10	0.10
WWR of east	0.2	0.12	0.12	0.14
Window height	3.0	3.4	3.4	3.4
Number of horizontal panels	10	16	16	16
Depth of louvers	7	9	9	9
Angle of louvers	0	−1	−1	−1
UDI (−%)	−72.59	−73.67	−72.91	−74.09
Cooling load (kWh/m^2)	176.58	163.01	162.87	163.38
PMV	1.13	0.83	0.82	0.84

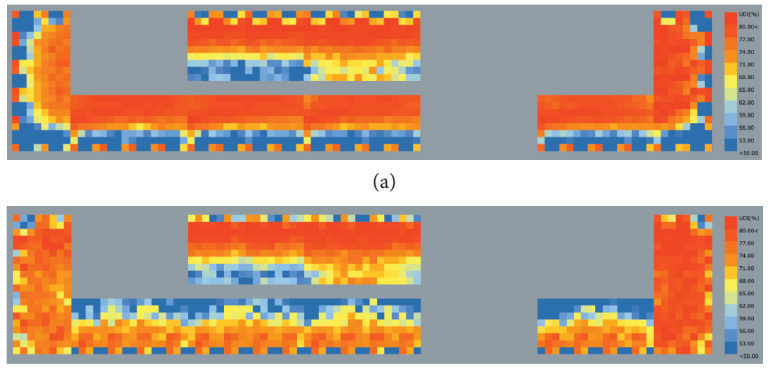

(a)

(b)

Figure 12: Visualization of UDI in the 7th floor office area before and after optimization. (a) UDI of initial solution and (b) UDI of Option 1.

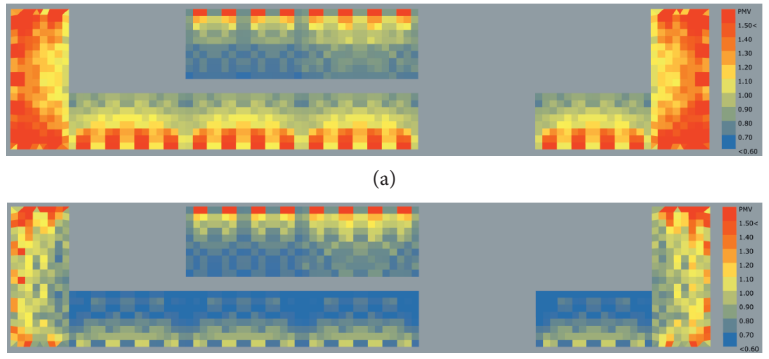

(a)

(b)

Figure 13: Visualization of PMV in the 7th floor office area before and after optimization. (a) PMV of initial solution and (b) PMV of Option 1.

Among the 116 samples obtained by the BP neural network, the broken-line diagram of predicted value basically coincides with the broken-line diagram of actual value, as can be seen from Figure 14. In Figure 15, it can be seen that the absolute error value of the BP neural network in Y_1 is within 6.65% and the maximum relative error is 12.80%, but both are within 15%, and the average relative error is 1.66%; the maximum absolute error of the BP neural network in Y_2 is 3.25 kwh/m^2, the maximum relative error is 1.75%, and the average relative error is only 0.27%; the maximum absolute error of the BP neural network in Y_3 is 0.12, the maximum relative error is 9.72%, and the average relative error is only 0.83%.

It can be concluded that, in the stages of the public building design scheme, the alternative model formed by the BP neural network achieves good prediction accuracy for the prediction of the cooling load, useful daylighting illumination, and thermal comfort, which also shows that the

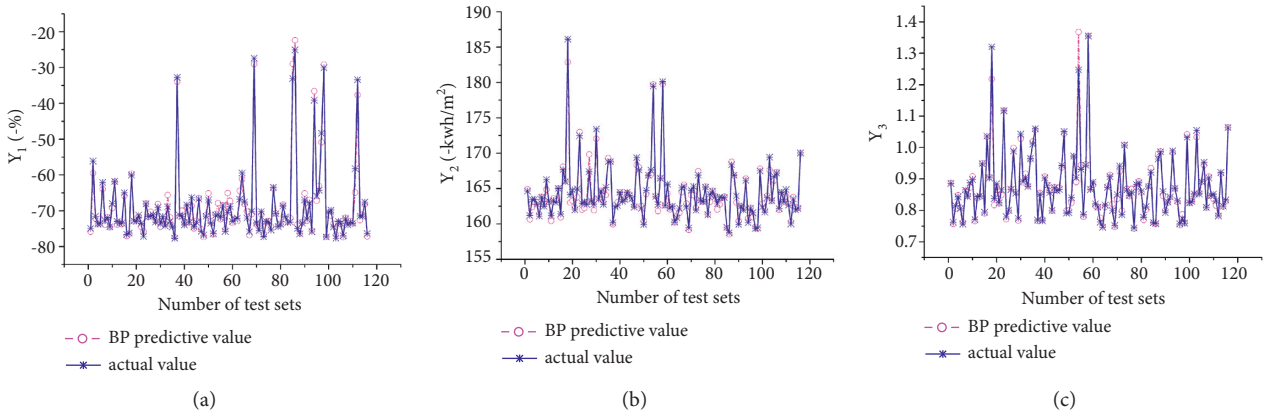

Figure 14: Predicted value and target value of BP neural network. (a) Y_1 represents UDI; (b) Y_2 represents cooling load; and (c) Y_3 represents PMV.

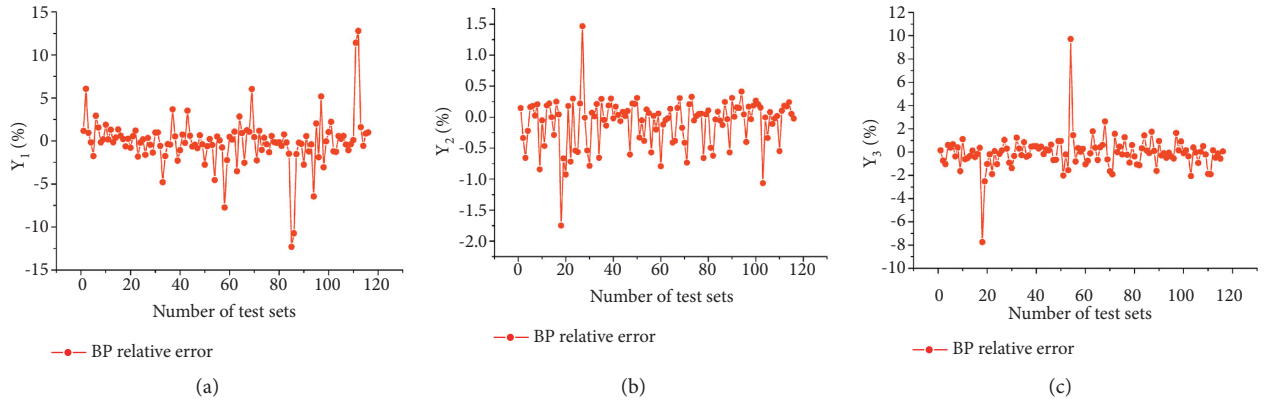

Figure 15: Fitting error percentage of BP neural network. (a) The relative error of Y_1 is relatively large, but it meets the requirements. (b) The relative error of Y_2 is relatively small. (c) The relative error of Y_3 is very small, except that one data value is 9.72%.

optimization method adopted in this paper is scientific and effective.

5. Conclusion

In the process of pursuing the development of building energy efficiency, passive design plays a vital role. In the design stage, the designer needs to achieve a balance between various optimization goals through the architectural design itself. The framework of "modeling simulation optimization prediction" is adopted for performing calculations. This paper proposed a multiobjective optimization model for the optimization of window opening and shading of a science and technology service center building in the tropical zone, so as to achieve a better balance between energy consumption, UDI, and PMV. The design variables used in the study included WWR, window height, and shading device size, which were optimized by a multiobjective genetic algorithm to generate a Pareto boundary, and provide multiple optimization solutions that meet these three objectives, so that the designer can choose the optimal solution based on these requirements.

Compared with the target value of the initial solution, the optimized target value obtains a more reasonable value. The results showed that the energy consumption decreased significantly, from 176.58 kwh/m^2 to 162.87–163.38 kwh/m^2, a decrease of 7.48–7.76%; the value of UDI increased slightly from 72.59% to 72.91%–74.09% and increased by 0.44%–2.07%; the PMV decreased from the initial 1.13 to 0.82–0.84. It was shown that the optimized office area achieved good improvement in energy consumption, daylighting, and thermal comfort, which can effectively realize the energy-saving optimization of the building. In the optimization process of decision variables, WWR had the greatest impact on decision variables, followed by louver variables. The WWR in the west, south, and east was reduced from 0.2 to 0.1, and the increase in horizontal panels and depth of louvers reduced the energy consumption to a lower value, achieving an ideal state of thermal comfort and, at the same time, caused UDI to reach a higher value.

Finally, this paper also introduced the combination of a BP neural network and a multiobjective evolutionary algorithm. Through the alternative model formed by the BP neural network, it achieved good prediction accuracy for the prediction of refrigeration load, useful daylighting illumination, and thermal comfort. Because Sanya has remarkable tropical characteristics, this paper considered Sanya as the research object, which put forward meaningful suggestions

for building energy conservation and sustainable development in Sanya.

Data Availability

Data used to support the findings of the study are listed within the article.

Conflicts of Interest

The authors declare that they have no conflicts of interest.

References

[1] T. Abergel, J. Dulac, I. Hamilton, M. Jordan, and A. Pradeep, *Global Status Report for Buildings and Construction towards a Zero-Emissions, Efficient and Resilient Buildings and Construction Sector*, Environment Programme, United Nations Environment Programme, 2019.

[2] BERCoT University, *Annual Report on China Building Energy Efficiency*, China Architecture & Building Press, Beijing, China, 2020.

[3] J. Zuo and Z.-Y. Zhao, "Green building research-current status and future agenda: a review," *Renewable and Sustainable Energy Reviews*, vol. 30, pp. 271–281, 2014.

[4] K. Perini, M. Ottelé, A. L. A. Fraaij, E. M. Haas, and R. Raiteri, "Vertical greening systems and the effect on air flow and temperature on the building envelope," *Building and Environment*, vol. 46, no. 11, pp. 2287–2294, 2011.

[5] R. T. Marler and J. S. Arora, "Survey of multi-objective optimization methods for engineering," *Structural and Multidisciplinary Optimization*, vol. 26, no. 6, pp. 369–395, 2004.

[6] A. A. S. Bahdad, S. F. S. Fadzil, H. O. Onubi, and S. A. BenLasod, "Multi-dimensions optimization for optimum modifications of light-shelves parameters for daylighting and energy efficiency," *International journal of Environmental Science and Technology*, vol. 18, 2021.

[7] A. Konak, D. W. Coit, and A. E. Smith, "Multi-objective optimization using genetic algorithms: a tutorial," *Reliability Engineering & System Safety*, vol. 91, no. 9, pp. 992–1007, 2006.

[8] K. Lee, K. Han, and J. Lee, "Feasibility study on parametric optimization of daylighting in building shading design," *Sustainability*, vol. 8, no. 12, pp. 1220–1236, 2016.

[9] A. Toutou, M. Fikry, and W. Mohamed, "The parametric based optimization framework daylighting and energy performance in residential buildings in hot arid zone," *Alexandria Engineering Journal*, vol. 57, no. 4, pp. 3595–3608, 2018.

[10] Y. Fang and S. Cho, "Design optimization of building geometry and fenestration for daylighting and energy performance," *Solar Energy*, vol. 191, pp. 7–18, 2019.

[11] B. Lartigue, B. Lasternas, and V. Loftness, "Multi-objective optimization of building envelope for energy consumption and daylight," *Indoor and Built Environment*, vol. 23, no. 1, pp. 70–80, 2014.

[12] A. Zhang, R. Bokel, A. van den Dobbelsteen, Y. Sun, Q. Huang, and Q. Zhang, "Optimization of thermal and daylight performance of school buildings based on a multi-objective genetic algorithm in the cold climate of China," *Energy and Buildings*, vol. 139, pp. 371–384, 2017.

[13] Y. Han, H. Yu, and C. Sun, "Simulation-based multiobjective optimization of timber-glass residential buildings in severe cold regions," *Sustainability*, vol. 9, no. 12, 2017.

[14] K. Lakhdari, L. Sriti, and B. Painter, "Parametric optimization of daylight, thermal and energy performance of middle school classrooms, case of hot and dry regions," *Building and Environment*, vol. 204, p. 17, 2021.

[15] L. Zhu, B. H. Wang, and Y. Sun, "Multi-objective optimization for energy consumption, daylighting and thermal comfort performance of rural tourism buildings in north China," *Building and Environment*, vol. 176, 2020.

[16] Y. Zhai, Y. Wang, Y. Huang, and X. Meng, "A multi-objective optimization methodology for window design considering energy consumption, thermal environment and visual performance," *Renewable Energy*, vol. 134, pp. 1190–1199, 2019.

[17] C. Sun, Q. Q. Liu, and Y. S. Han, "Many-objective optimization design of a public building for energy, daylighting and cost performance improvement," *Applied Sciences-Basel*, vol. 10, no. 7, 2020.

[18] J. Zhao and Y. Du, "Multi-objective optimization design for windows and shading configuration considering energy consumption and thermal comfort: a case study for office building in different climatic regions of China," *Solar Energy*, vol. 206, pp. 997–1017, 2020.

[19] Y. Yau and B. Chew, "A review on predicted mean vote and adaptive thermal comfort models," *Building Service Engineering Research and Technology*, vol. 35, no. 1, pp. 23–35, 2014.

[20] S. Foster, *Improved thermal comfort for Hawai'i's as Elementary Schools: Designing an Educational Building for thermal comfort Using Passive Design Techniques in the Hot and Humid Climate*, University of Hawaii, Hawaii, America, 2021.

[21] I. A. Basheer and M. Hajmeer, "Artificial neural networks: fundamentals, computing, design, and application," *Journal of Microbiological Methods*, vol. 43, no. 1, pp. 3–31, 2000.

[22] A. Nabil and J. Mardaljevic, "Useful daylight illuminance: a new paradigm for assessing daylight in buildings," *Lighting Research and Technology*, vol. 37, no. 1, pp. 41–57, 2005.

[23] B. Zhou, *Research on Multi-Objective Optimization of Multilayer Office Building Space in Cold Region Based on Daylight Performance*, Harbin Institute of Technology, Harbin, China, 2017.

[24] H. Liu, X. Ma, Z. Zhang, X. Cheng, Y. Chen, and S. Kojima, "Study on the relationship between thermal comfort and learning efficiency of different classroom-types in transitional seasons in the hot summer and cold winter zone of China," *Energies*, vol. 14, no. 19, 2021.

[25] W. Gang, S. Wang, K. Shan, and D. Gao, "Impacts of cooling load calculation uncertainties on the design optimization of building cooling systems," *Energy and Buildings*, vol. 94, pp. 1–9, 2015.

[26] *DBJ46–03–2017, "Design Standard for Energy Efficiency of Public Buildings in Hainan*, China Architecture & Building Press, Beijing, China, 2017.

[27] A. I. Palmero-Marrero and A. C. Oliveira, "Effect of louver shading devices on building energy requirements," *Applied Energy*, vol. 87, no. 6, pp. 2040–2049, 2010.

[28] *GB50033–2013, "Standard For Daylighting Design of Buildings*, China Architecture & Building Press, Beijing, China, 2013.

[29] *GB50176–2016, "Code For thermal Design of Civil Building*, China Architecture & Building Press, Beijing, China, 2016.

[30] Y. Luo, *A Research on the Process of Building Performance Optimization Based on Parametric Design Platform*, Tianjin University, Tianjin, China, 2017.

[31] J. Zhang, L. Ji, and H. X. Li, "Optimization of daylighting, ventilation, and cooling load performance of apartment in tropical ocean area based on parametric design," *Advances in Civil Engineering*, vol. 2021, pp. 1–11, 2021.

[32] Q. S. Ma and H. Fukuda, "Parametric office building for daylight and energy analysis in the early design stages," *Conference on Urban Planning and Architectural Design for Sustainable Development*, vol. 216, pp. 818–828, 2016.

[33] F. Soflaei, M. Shokouhian, A. Tabadkani, H. Moslehi, and U. Berardi, "A simulation-based model for courtyard housing design based on adaptive thermal comfort," *Journal of Building Engineering*, vol. 31, p. 12, 2020.

[34] J. Rana, R. Hasan, H. R. Sobuz, and V. W. Y. Tam, "Impact assessment of window to wall ratio on energy consumption of an office building of subtropical monsoon climatic country Bangladesh," *International Journal of Construction Management*, pp. 1–26, 2020.

[35] P. Xue, Q. Li, J. Xie, M. Zhao, and J. Liu, "Optimization of window-to-wall ratio with sunshades in China low latitude region considering daylighting and energy saving requirements," *Applied Energy*, vol. 233-234, no. 234, pp. 62–70, 2019.

[36] H. Huo, W. Xu, A. Li, Y. Lv, and C. Liu, "Analysis and optimization of external Venetian blind shading for nearly zero-energy buildings in different climate regions of China," *Solar Energy*, vol. 223, pp. 54–71, 2021.

[37] N. Nasrollahzadeh, "Comprehensive building envelope optimization: improving energy, daylight, and thermal comfort performance of the dwelling unit," *Journal of Building Engineering*, vol. 44, pp. 103–418, 2021.